


## Boltzmann-distribution-equivalent for Lévy noise and how it leads to thermodynamically consistent epicalysis

Martin Bier\*

*Department of Physics, East Carolina University, Greenville, North Carolina 27858, USA*

 (Received 3 August 2017; revised manuscript received 22 October 2017; published 12 February 2018)

Nonequilibrium systems commonly exhibit Lévy noise. This means that the distribution for the size of the Brownian fluctuations has a “fat” power-law tail. Large Brownian kicks are then more common as compared to the ordinary Gaussian distribution. We consider a two-state system, i.e., two wells and a barrier in between. The barrier is sufficiently high for a barrier crossing to be a rare event. When the noise is Lévy, we do not get a Boltzmann distribution between the two wells. Instead we get a situation where the distribution between the two wells also depends on the height of the barrier that is in between. Ordinarily, a catalyst, by lowering the barrier between two states, speeds up the relaxation to an equilibrium, but does not change the equilibrium distribution. In an environment with Lévy noise, on the other hand, we have the possibility of epicalysis, i.e., a catalyst effectively altering the distribution between two states through the changing of the barrier height. After deriving formulas to quantitatively describe this effect, we discuss how this idea may apply in nuclear reactors and in the biochemistry of a living cell.

DOI: [10.1103/PhysRevE.97.022113](https://doi.org/10.1103/PhysRevE.97.022113)

### I. INTRODUCTION

A good understanding exists of how the characteristics of Brownian motion and thermal noise at the microscopic level translate into a Boltzmann distribution at the macroscopic level [1,2]. However, all these results apply solely for a system that is at equilibrium. Most of the systems of interest for physicists, however, are far from equilibrium. Solar physics, biophysics, geophysics, etc., are all about systems that convert, transport, and dissipate energy. Being far from equilibrium is the very essence of these systems.

Already in the early 1900s it was discovered that the noise that is exhibited by systems that are far from equilibrium is fundamentally different from the noise that is exhibited by equilibrium systems [3]. To date many features of nonequilibrium noise are still not fully understood and nonequilibrium thermodynamics is still very much a work in progress.

Also in the early part of the 20th century, mathematicians developed theory for probability distributions with infinite variance. The Cauchy distribution,  $p(x) = \pi/(1+x^2)$ , is a good example. The infinite variance of this distribution is associated with the asymptotic behavior: in the  $x \rightarrow \pm\infty$  limit we have  $p(x) \propto 1/x^2$ . Such a power-law tail is much more “fat” than the tail of the Gaussian distribution [which follows  $p(x) \propto \exp[-x^2/2\sigma^2]$ , where  $\sigma$  is the standard deviation]. The fat tail means that large  $x$ ’s, i.e., extreme events, are more common when a sequence of numbers is generated.

This mathematical work acquired real-life significance when Mandelbrot discovered in the 1960s that the price increments of cotton futures exhibit a fat tail [4].

It takes lots of data and data processing to definitively identify a tail as deriving from a power law. But in the 1990s desktop computers became sufficiently fast and easy to use that

identifying power-law tails could become a cottage industry [5–7]. “Noise with pulsatory outbursts” appears to be inherent to phenomena far from equilibrium.

There is currently much research interest in the nonequilibrium nature of the living cell. The focus is on identifying nonequilibrium noise [8], as well as on exploring consequences of nonequilibrium activity [9]. Below we will derive and explore a remarkable effect of nonequilibrium activity.

### II. WHITE GAUSSIAN NOISE IN AN EQUILIBRIUM SYSTEM

The one-dimensional Langevin equation describes an overdamped particle in a potential  $V(x)$  that is subject to Brownian kicks:

$$\dot{x} = -\gamma \frac{dV(x)}{dx} + \sqrt{2D}\xi(t). \quad (1)$$

Here  $\gamma$  represents the mobility of the particle in the medium. The mobility is the emergent ratio  $\gamma = v/F$  when a force  $F$  is applied and an average speed  $v$  through the medium results. The noise term  $\sqrt{2D}\xi(t)$  describes the Brownian kicks.  $D$  is here the diffusion coefficient of the particle. For equilibrium systems the noise  $\xi(t)$  is generally taken to be white and Gaussian [2]. The noise term  $\xi(t)$  is normalized through  $\langle \xi(t)\xi(t') \rangle = \delta(t-t')$ , where  $\delta(t-t')$  represents a Dirac delta function. At equilibrium there exists a relation to connect the noise strength and the mobility:  $D = k_B T \gamma$ . Here  $k_B$  is Boltzmann’s constant and  $T$  is the absolute temperature. This is Einstein’s well-known fluctuation dissipation theorem (FDT). At the end of Sec. IV we will let the variable  $x$  in Eq. (1) represent the reaction coordinate of a chemical reaction. Equation (1) itself then describes the advance of the chemical reaction.

The “white” part of the equilibrium noise means that there is no correlation between subsequent values  $\xi(t)$  and  $\xi(t + \Delta t)$  on even the smallest resolvable time scale  $\Delta t$ . For the noise to be genuinely “white,”  $\xi(t)$  thus needs to be fractal [10].

\*bierm@ecu.edu

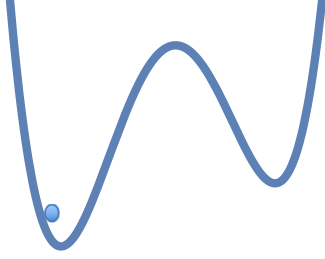


FIG. 1. A double-well potential. Equation (1) describes the dynamics of an overdamped Brownian particle in the potential.

The scaling law  $\xi(\lambda t) = \lambda^{-1/2}\xi(t)$  describes the self-similar structure.

It is through  $\sqrt{2D}\xi(t) = \xi(t/2D)$  and  $t' = t/2D$  that the factor  $\sqrt{2D}$  can be absorbed in the time scale. Let  $\xi(t')$  have a standard deviation  $\sigma = 1$  when time steps of unit length are taken. In that case a discretization of Eq. (1) with time intervals of  $\Delta t'$  requires at each time step a contribution  $\xi(t'_m) = \theta_m/\sqrt{\Delta t'}$ , where  $m$  enumerates the time steps and  $\theta_m$  represents a number drawn from a zero-average Gaussian distribution with a standard deviation of 1. This also leads to  $\langle \xi^2(t'_m) \rangle = 1/\Delta t'$ . Through  $\Delta x/\Delta t' = \theta_m/\sqrt{\Delta t'}$  we next retrieve the well-known diffusion result  $\langle \Delta x^2 \rangle = 2D\Delta t$  that holds for constant  $V(x)$  in Eq. (1) and that is valid for all  $\Delta t$ .

The ‘‘Gaussian’’ part of the equilibrium noise refers to the distribution  $p(\xi)$  of the kick sizes. In liquid water at room temperature a water molecule undergoes about  $10^{12}$  collisions per second with other water molecules. The central limit theorem tells us that the cumulative effect of multiple stochastic inputs converges to a Gaussian distribution [2]. An important condition here is that all these ‘‘stochastic inputs’’ have a finite variance. If that condition is satisfied, the Gaussian is the ‘‘attractor.’’ When combining probability distributions to obtain a cumulative effect, the convergence to a Gaussian is generally rapid. In the aforementioned liquid-water environment this means that at any time scale that is about an order of magnitude larger than  $10^{-12}$  s (the time between subsequent collisions) a Gaussian distribution is a good approximation for the total distance covered by a particle due to collisions with surrounding water molecules. A Gaussian distribution,  $p(\xi) \propto \exp[-\xi^2/2\sigma^2]$ , where  $\sigma$  represents the standard deviation, has a tail that converges rapidly and makes all moments converge.

The stochastic ordinary differential equation, Eq. (1), can be written as an equivalent nonstochastic partial differential equation for the time evolution of the probability distribution,  $P(x,t)$ , of the Brownian particle in the potential

$$\partial_t P(x,t) = \gamma \partial_x \{ [\partial_x V(x)] P(x,t) \} + D \partial_x^2 P(x,t). \quad (2)$$

Here the subscripts denote the taking of a partial derivative with respect to that variable. From Eq. (2) and the FDT ( $D = k_B T \gamma$ ) it is straightforward to derive that the stationary distribution ( $\partial_t P = 0$ ) is a Boltzmann distribution, i.e.,  $P(x) \propto \exp[-V(x)/k_B T]$  [1].

Consider particles near a minimum in the potential drawn in Fig. 1. The low noise limit means that the difference between the barrier height  $E_{\max}$  and the minimum  $E_{\min}$  is sufficiently large for noise-activated escape from a well to be rare. For that case it is straightforward to derive that the particles’ escape

rate over the barrier follows  $k \propto \exp[-(E_{\max} - E_{\min})]$ , where  $E_{\max}$  and  $E_{\min}$  are expressed in units of  $k_B T$  [1,11].

### III. NONEQUILIBRIUM NOISE AND ITS NUMERICAL ISSUES

As was mentioned in the Introduction, a system that is far from equilibrium commonly exhibits noise with more ‘‘extreme events.’’ In the same way that the Gaussian distribution is the attractor for distributions with a finite variance, the so-called alpha-stable or Lévy distribution is the attractor for distributions with a diverging variance, i.e.,  $\langle \xi^2(t) \rangle \rightarrow \infty$  [12,13]. For that reason, Lévy noises arise naturally in the description of random processes with large outliers

There is an analytic expression for the ‘‘kicksize’’ distribution  $p_\alpha(\xi)$  of symmetric Lévy noise [14]. However, this expression is complicated and involves generalized hypergeometric functions. Working with the more concise expression for the associated characteristic function [ $\tilde{p}_\alpha(k) \equiv \int p_\alpha(\xi) \exp[ik\xi] d\xi$ ] is generally more effective. For the characteristic function of the symmetric, zero-average Lévy distribution we have

$$\tilde{p}_\alpha(k) = \exp[-\sigma^\alpha |k|^\alpha]. \quad (3)$$

Here  $\sigma$  is a scale parameter that gives the intensity of the noise. The parameter  $\alpha$  ( $0 < \alpha \leq 2$ ) is the stability index. For  $\alpha = 2$  the case of finite variance and ensuing Gaussian distribution is retrieved. The parameter  $\sigma$  represents in that case the standard deviation divided by  $\sqrt{2}$ . For  $\alpha = 1$  the aforementioned Cauchy noise is obtained.

With Gaussian noise, tails are rapidly decaying and follow  $p_2(\xi) \propto \exp[-\xi^2/4\sigma^2]$ . But for  $\alpha < 2$  we have a probability density distribution with a ‘‘fat’’ power-law tail,  $p_\alpha(\xi) \propto |\xi|^{-(1+\alpha)}$ . Note that such a fat tail leads to a diverging variance for the distribution.

The divergence of  $\langle \xi^2(t) \rangle$  complicates the mathematical analysis. There is, for instance, no longer an FDT. However, as we will see, there are features that are more easily evaluated with distributions that have power-law tails.

Consider activated escape over the barrier depicted in Fig. 1. We take a barrier that is, compared to the noise amplitude, sufficiently high for barrier crossings to be rare events. Both for Gaussian and for Lévy noise, the low-noise limit means that barrier crossings involve ‘‘unlikely’’ kicks from the tail of the distribution. The most probable escape path (MPEP) is the most likely sequence among the unlikely sequences that lead to barrier crossing.

For a system at equilibrium, microscopic reversibility must hold. Microscopic reversibility [15] means that every trajectory on the potential is traversed just as often as its time reverse. So if a movie were made of a Brownian particle on the potential, there would be no way to determine whether such a movie is played forward or backward. This implies that, at equilibrium, the MPEP for a particle in the potential in Fig. 1 must be the reverse of the most probable way to slide down from the top of the barrier. Both the Gaussian white noise and the Lévy white noise that we consider in this article have a distribution with a central maximum at  $\xi = 0$ , i.e.,  $\xi = 0$  is the most likely kick size. This means that the most likely downslide from the barrier, even in the noisy environment, is actually the deterministic one described by  $\dot{x} = -dV(x)/dx$ . For a system

at equilibrium this implies that the most likely trajectory up the barrier is the time reverse of the noiseless “slide” down the barrier. In an elegant paper, Onsager and Machlup proved rigorously that this feature of microscopic reversibility also follows from the statistical properties of Gaussian noise [16].

That the most likely stochastically driven upslide is the reverse of the deterministic downslide adds the downslide time  $\tau$  as a characteristic time to a barrier [17,18]. The other characteristic time is, of course, the average time spent in a well before an escape over the barrier occurs. In a Euler-scheme simulation of a particle in an equilibrium environment on the potential in Fig. 1, we discretize the trajectory, i.e.,  $x(t_{m+1}) = x(t_m) + \Delta x_m$ , and, after scaling away parameters, we compute increments  $\Delta x$  using

$$\Delta x_m = \{-V'[x(t_m)] + \xi(t_m)\}\Delta t. \quad (4)$$

For a simulation to be accurate, we need to take  $\Delta t \ll \tau$ , i.e., take time steps that are much smaller than this characteristic time  $\tau$ . This means that the MPEP will involve a *sequence* of steps; subsequent kicks will “conspire” to bring the particle over the barrier. The idea of the Euler scheme is that these subsequent kicks are small straight segments  $(\Delta t, \Delta x)$ . For the Euler scheme to be accurate, the covered  $\Delta x_i$ ’s should be sufficiently small that no appreciable change of  $V'(x)$  occurs along one segment.

All in all, when the noise is Gaussian, the movement of a noisy particle on a potential can be adequately described with a traditional Euler scheme. Any desired accuracy can be obtained by taking sufficiently small time intervals and taking sufficiently many digits in the involved numbers.

When the noise is Lévy, the situation is fundamentally different. With Lévy noise we are no longer in equilibrium and there is no microscopic reversibility [19]. It has been rigorously shown that, in the case of Lévy noise, the MPEP over a barrier derives from just *one kick* [19,20]. No longer is there a characteristic time associated with the MPEP.

In terms of Fig. 1 and a simulation this means that the indicated particle at the bottom of the well will do the entire escape trajectory over the well in one time step  $\Delta t$ . Of course, the idea that the force due to the potential is constant during this time step is then no longer valid; the force at the indicated initial position is in the positive direction and the entire concept of mounting a barrier no longer applies. The curvature of the potential in the course of a time step is no longer negligible.

This problem cannot be overcome by taking smaller time steps. With a smaller value of  $\Delta t$ , the probability of escape at a particular time step will be smaller. However, there are correspondingly more time steps in a unit of time and the transition rate across the barrier (the probability of escape per unit of time) will stay the same.

In our approach we overcome the curvature problem by taking a piecewise linear potential as in Fig. 2. When the corner at the top of the barrier is crossed in the course of a time step, then the deterministic force changes abruptly in the middle of a step. Potentials with corners can often give rise to behavior that is qualitatively different from that on smooth potentials. However, noise tends to “smooth out” corners and when noise is present, piecewise linear potentials no longer exhibit unique features.

With the piecewise linear potential we are no longer approximating a curved potential with linear segments. This

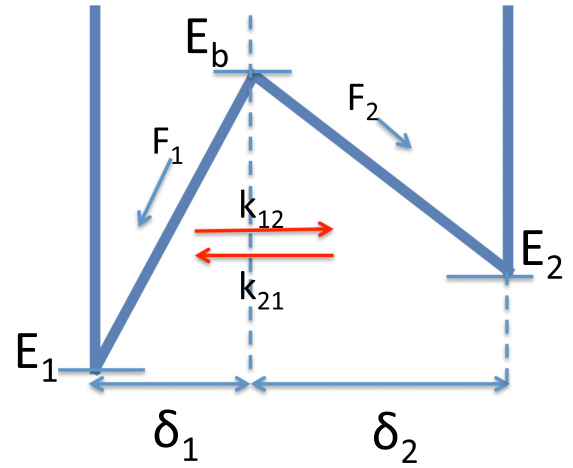


FIG. 2. The piecewise-linear, double-well potential that we use as the basis for our analysis. The energy levels of the left well, the barrier, and the right well are  $E_1$ ,  $E_b$ , and  $E_2$ , respectively. The widths of well 1 and well 2 are  $\delta_1$  and  $\delta_2$ , respectively.  $F_1$  and  $F_2$  are the deterministic forces driving a particle toward the bottom. The transition rates are  $k_{12}$  and  $k_{21}$ .

eliminates a source of inaccuracy. However, it should be realized that with the way we handle the corner, there still is inaccuracy. We take  $\xi(t)\Delta t$  as the displacement due to a kick, but in actuality  $\xi(t)$  is a fractal and has structure on all scales. Therefore  $\xi(t)\Delta t$  is the result of a “hairy trajectory.” Neglecting this “hairiness” and treating the corner the way we do, we are effectively taking a mean-field approach for the barrier crossing.

Consistent with the overdamped assumption, we let the particle come to an immediate standstill when it hits one of the vertical barriers on the left or right edge of the potential. There is no “bouncing.” Once the particle is at the position of the vertical barrier, only a kick in the opposite direction, away from the barrier, can possibly move it.

#### IV. RATES AND DISTRIBUTIONS FOR THE DOUBLE WELL WITH LÉVY NOISE

With the barrier sufficiently high, a particle in the potential depicted in Fig. 2 will spend most of its time near or at the bottom of a well. Suppose the minimal required kick size to get from the bottom of a well to across the barrier is  $\xi_0$ , where  $\xi_0 > 0$ . With  $p_\alpha(\xi) \propto \xi^{-(1+\alpha)}$  for the right tail of the probability distribution, we have for the probability of a kick larger than  $\xi_0$ ,

$$P(\xi > \xi_0) = \int_{\xi_0}^{\infty} p_\alpha(\xi) d\xi \propto \xi_0^{-\alpha}. \quad (5)$$

The starting point for the analysis in this section is the potential sketched in Fig. 2. The level of the barrier in Fig. 2 is  $E_b$ . The minimum on the left corresponds to an energy  $E_1$  and the minimum on the right corresponds to an energy  $E_2$ . The transition rate from the  $E_1$  well to the  $E_2$  well is  $k_{12}$  and the transition rate from the  $E_2$  well to the  $E_1$  well is  $k_{21}$ . At steady state we have for the ratio of the times  $P_1$  and  $P_2$  spent in the

first and second well

$$\frac{P_2}{P_1} = \frac{k_{12}}{k_{21}}. \quad (6)$$

With a large population of particles in the double well, the ratio  $P_2/P_1$  tells us how, in steady state, the particles are distributed over the two wells.

For the potential in Fig. 2 we have

$$\left| \frac{dV(x)}{dx} \right| = F_i = \frac{E_b - E_i}{\delta_i}, \quad (7)$$

where  $i = 1, 2$ . We take  $\beta = 1/\gamma$  as the coefficient of friction that is associated with the overdamped motion in the potential. We then derive from Eq. (1) that for a kick  $\xi_{0,i}$  to lead to a barrier crossing  $i \rightarrow j$  it is required that

$$\beta(-1)^{i+1}\xi_{0,i} \gtrsim \left[ \frac{\beta\delta_i}{\Delta t} + \frac{E_b - E_i}{\delta_i} \right]. \quad (8)$$

The probability of occurrence of such a kick [cf. Eq. (5)] is proportional to the transition rate out of well  $i$ . We thus have

$$k_{ij} \propto \left[ \frac{\beta\delta_i^2}{\Delta t} + (E_b - E_i) \right]^{-\alpha}. \quad (9)$$

Here the first term on the right-hand side of Eq. (9) represents the amount of energy that is necessary to overcome friction. The second term on the right-hand side is the energy that is necessary to bring the particle from the bottom to the top of the barrier in Fig. 2.

A chemical reaction is commonly depicted with the aid of a potential as in Fig. 1 [21]. The minima then correspond to identifiable chemical states like the “chair” and “boat” states of cyclohexane or the “open and “closed” states of an ion channel. The maxima then correspond to the activation barriers that separate these states and the variable  $x$  is called a “reaction coordinate.” For an individual molecule in a thermal bath, the reaction kinetics is next viewed as the overdamped Brownian motion of a particle along the  $x$  axis.

However, the reaction coordinate, as in Figs. 1 and 2, is an abstraction. The position of a point along a reaction coordinate is a measure for how far a chemical transition has advanced. Only in a very few cases can this position be related to something concrete. In a later section we will use recently obtained data on DNA folding and see a case where we can quantitatively assess both terms on the right-hand side of Eq. (9). The folding of DNA, RNA, and proteins offers one of the few instances where the progress of a transition can be expressed in terms of nanometers.

Another issue concerns the  $\Delta t$  in Eq. (9). Also for Lévy noise the function  $\xi(t)$  is a fractal, i.e., a mathematical object with structure on all scales. When modeling systems with noise, we generally take  $\Delta t$  smaller than any characteristic time of the system. For an overdamped particle subjected to Gaussian white noise in a potential as in Fig. 1, this means that we have to take a  $\Delta t$  that is significantly smaller than the time to complete the MPEP. If the noise is Lévy, however, the time  $\Delta t$  is also the characteristic time for the MPEP. In that case the physics that underlies the noise needs to be invoked to set the limit on  $\Delta t$ . As was mentioned before, in an aqueous medium at room temperature a water molecule’s time between successive collisions is of picosecond order of magnitude. A simulation

with a  $\Delta t$  that is smaller than a picosecond is therefore no longer realistic.

## V. EPICATALYSIS

A catalyst is a substance that lowers the activation barrier ( $E_b$  in Fig. 2) while leaving unchanged the energy levels of the states on either side of the barrier ( $E_1$  and  $E_2$  in Fig. 2) [21]. It thereby speeds up the relaxation to a Boltzmann equilibrium between the two states in a double-well potential. The catalyst has no interaction with the states to the left and right of the maximum that it lowers. Without the presence of catalyzing enzymes most biochemical processes have activation barriers that are too high for the process to occur within the necessary time span. A catalyst is only involved in the conversion from reactant into product. It operates as a “transfer station” that itself remains unaltered by the process. Generally, very little catalyst is required to significantly speed up a reaction.

Epicalysis is a form of catalysis in which the catalyst changes the steady-state distribution between the reactant state and the product state [22,23]. For a Boltzmann equilibrium the steady-state distribution can only be modified by changing the energy difference between reactant state and product state. By merely changing the height of an activation barrier, a catalyst *cannot* affect the Boltzmann equilibrium. Figure 3 is in the spirit of Maxwell’s Demon [24] and shows once more how epicalysis is impossible in a closed system that is only allowed to equilibrate: if epicalysis were real, it would imply the possibility of violating the first law of thermodynamics. Such violation would permit the construction of a perpetual mobile. In an equilibrium environment the presence of a catalyst cannot change the steady-state distribution.

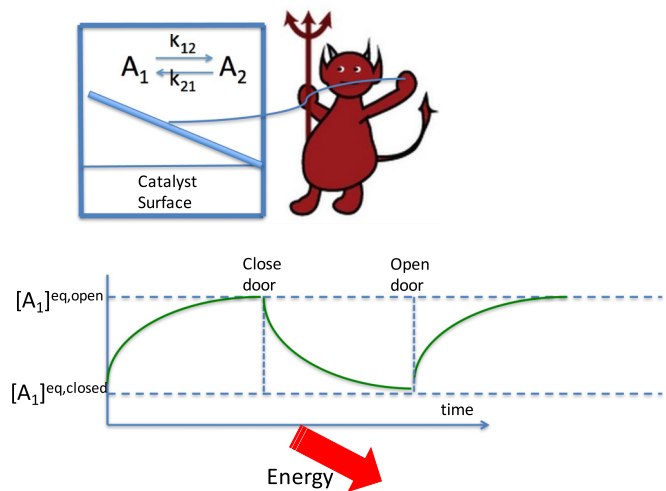


FIG. 3. A setup to illustrate that epicalysis in a closed environment is absurd as it leads to the possibility of a perpetual mobile. A simple monomolecular reaction,  $A_1 \rightleftharpoons A_2$ , is taking place in a sealed container. A weightless and frictionless trapdoor is repeatedly opened and closed by a demon. When the trapdoor is open, the reactants and products in the container are exposed to a catalyst. If the catalyst changes the Boltzmann distribution, then the system moves to a new equilibrium after every opening or closing of the trapdoor. As energy can be extracted from such equilibration, the setup is obviously nonsensical.



Below we will show how epicalysis is possible if the Brownian kicks that are driving the barrier crossings are drawn from a Lévy distribution. Lévy noise occurs when a system is open and kept out of equilibrium. A system can be in an out-of-equilibrium steady state when energy comes into the container in one form and is converted and/or transferred before it leaves the container at the same rate [25]. Inside the container, energy is then dissipated and entropy is produced. If such nonequilibrium is maintained in the container of Fig. 3, the activity of the demon simply redirects some of the energy flow; no violation of the first law occurs in that case.

From Eqs. (6) and (9) we have

$$\frac{P_2}{P_1} = \frac{k_{12}}{k_{21}} \propto \left[ \frac{\frac{\beta \delta_2^2}{\Delta t} + (E_b - E_2)}{\frac{\beta \delta_1^2}{\Delta t} + (E_b - E_1)} \right]^\alpha. \quad (10)$$

If we neglect the friction terms, the  $E_b$  dependence becomes more salient:

$$\frac{P_2}{P_1} \propto \left( \frac{E_b - E_2}{E_b - E_1} \right)^\alpha. \quad (11)$$

In Eqs. (10) and (11) a “proportional to” symbol is used. The prefactor that would be there in the case of an “=” sign is a function of the ratio of the widths of the wells. It is remarkable that the  $E_b$  features in these equations. With Gaussian white noise we have for the transition rates  $k_{12} \propto \exp[-(E_b - E_1)]$  and  $k_{21} \propto \exp[-(E_b - E_2)]$ . For the steady-state distribution,  $P_2/P_1 = k_{12}/k_{21}$ , we then find that the  $E_b$  cancels out:  $P_2/P_1 \propto \exp[-(E_2 - E_1)]$ . The  $E_b$  does *not* cancel out when the transition rates follow power laws as in Eq. (9). The  $E_b$  dependence of the steady-state distribution  $P_2/P_1$  is what makes it possible for the demon in Fig. 3 to extract energy if the fluid in the beaker is kept out of equilibrium.

For large  $E_b$ , the ratio on the right-hand side in Eqs. (10) and (11) approaches unity. The presence of a catalyst lowers the activation energy  $E_b$  and thus drives the system away from the unity ratio. A lower  $E_b$  leads to a larger fraction of the total population going into the lower well. The effect is most prominent in Eq. (11). The friction terms in Eq. (10) mitigate the effect, but do not eliminate it.

As was mentioned before, the Lévy noise that is required for epicalysis is generally found in systems that are far from equilibrium. Lévy noise is, for instance, used in models for the time evolution of the Earth’s climate [26]. Such an approach is sensible as the Earth’s surface facilitates a continuous conversion of energy: it receives sunlight that is mostly in the visible part of the spectrum and emits energy at the same rate in the form of mostly infrared light. As already mentioned, the first time that Lévy noise was shown in empirical data occurred in the 1960s in the context of the study of cotton-future prices [4]. Of course, any economic activity is far from equilibrium as goods and services flow in one direction and money flows in the opposite direction. Life itself is a far-from-equilibrium phenomenon and it is therefore not surprising that Lévy statistics has been found in the time intervals between subsequent heartbeats [5] and in other physiological processes [27].

Only recently has it become possible to experimentally follow mechanical noise in a living cell on the molecular scale [28,29]. It has been found that cytoplasmic mechanical activity

is far from equilibrium and that the total noise intensity far exceeds the basic thermal  $k_B T$  level. With small probes it has furthermore been found that the large fluctuations that are typical for Lévy statistics occur in both cytoskeletal networks and in surrounding cytoplasmic fluid [30,31]. The picture that emerges from these latter results is one where the living cell is a setting with Boltzmann stationarity and added pulses that bring about the fat power-law tails and the Lévy behavior. The living cell constitutes a setting in which the epicalysis described in this section may be ubiquitous.

Consider again a double-well potential as in Figs. 1 and 2. In an equilibrium environment, with or without a catalyst, rates follow an Arrhenius relation, i.e.,  $k \propto \exp[-\Delta E/k_B T]$  [21]. Furthermore, the ratio of the forward and backward transition rates has a simple exponential, Boltzmann dependence on the inverse temperature and on the energy difference between the minima. If the aforementioned added Lévy pulses are present and responsible for a significant fraction of the transitions, then the Arrhenius plot,  $\log k$  vs  $1/T$ , is no longer a simple straight line. The transition-rate ratio, moreover, will then be more complicated than the Boltzmann exponential and carry a dependence on  $E_b$ .

The rates of nuclear fusion reactions in a plasma environment have commonly been estimated assuming a Maxwell-Boltzmann velocity distribution in the plasma. In such a setting a reaction will occur if reactants collide with sufficient energy to overcome a Coulomb barrier, i.e., in the case of an extreme event from the tail of the distribution. These plasmas, however, are out of equilibrium because of the very processes that bring about the high temperature in the first place. It is by now well established that fluctuations in plasmas follow Lévy statistics [32,33]. With this idea Ebeling and Romanovsky could quantitatively account [34] for the free neutron output in a fusion experiment with a deuteron plasma [35]. In that experiment the neutron output turned out about ten times as high as predicted by the assumption of a plasma at a Boltzmann equilibrium.

Catalysis is common in nuclear reactions. The CNO (carbon-nitrogen-oxygen) cycle is a catalyzed form of hydrogen fusion that is prominent in heavy stars [36]. In muon-catalyzed fusion the hydrogen molecules are made smaller through the replacement of an electron by a muon. The ensuing closer proximity of the nuclei allows for thermonuclear fusion with significantly lower activation barriers [37,38].

Fat tails and catalysis are prevalent in nuclear reactions. The discussed epicalysis could thus be significant for understanding and controlling the steady-state operation of contained, self-sustaining, nuclear chain reactions.

## VI. APPLICATION TO DNA FOLDING

For DNA strands the energy difference between the folded state and the unfolded state is such that the strand is effectively stuck in the folded state. In 2012 researchers connected the two ends of a DNA strand to silica beads [39]. Next they used optical traps to apply a force toward extension of the strand. With the added bias due to that force, the folded state and the unfolded state were of comparable energy. Tracking the distance between the beads, the researchers could next follow the fluctuations between the folded and unfolded state.

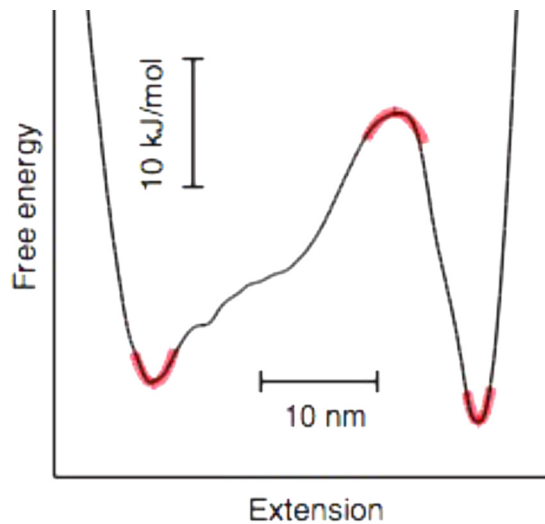


FIG. 4. From Ref. [39]. The reaction coordinate for one of the studied DNA strands. The wells correspond to the folded and unfolded states.

The distance between the beads sets up a reaction coordinate. Assuming that the observed distribution of distances is a Boltzmann distribution on a potential, a profile along the reaction coordinate can be constructed (Fig. 4).

The gathered data in Ref. [39] allow for the determination of the diffusion coefficient  $D$  and of the time  $\tau$  that it takes to transition from one state to the other. For  $D$  a value of around  $10^{-12}$  m<sup>2</sup>/s is found. With the FDT ( $\beta = k_B T/D$ ), we can use  $D$  to estimate the coefficient of friction  $\beta$ . For the transition time  $\tau$  (which is the time to complete a MPEP) values of around 10  $\mu$ s are found. If we view an *in vivo* system as one where there is external “Lévy forcing” in an environment with a thermal bath and an FDT, then we can take  $\Delta t \approx \tau$  as an upper limit for the increments associated with the Lévy noise. These estimates, together with estimates for the energies and distances derived from Fig. 4, can next be substituted in Eq. (9). It is then found that the friction term and the potential energy term are of similar magnitude. This means that in the presence of Lévy noise, the steady-state distribution should discernibly depend on the barrier height [cf. Eq. (10)]. Epicatalysis could thus be a noticeable effect in folding. *In vivo* the folding of DNA, RNA, and protein is commonly catalyzed. A catalyst bringing down the energy barrier would further bias the steady-state distribution to the one with the lower energy. In

the context of Fig. 4 this means that bringing down the barrier shifts the population balance toward the lower well on the right.

## VII. DISCUSSION

Lévy noise has been identified in many out-of-equilibrium systems. There is no simple general theory to explain why Lévy noise emerges in an out-of-equilibrium system. But a good understanding can be developed of how the presence of Lévy noise leads to many standard equilibrium characteristics no longer being valid [19]. In this article it has been shown how stationary distributions over states are different from the traditional Boltzmann distribution if the noise in a system is Lévy distributed. One of most salient consequences is that, in a nonequilibrium environment, a catalyst can change a steady-state distribution by changing the height of an activation barrier of a reaction.

The mechanism described above could be relevant for our understanding of a living cell. A network of chemical reactions may proceed differently in an *in vitro* equilibrium environment as compared to how it proceeds in the far-from-equilibrium living cell. In Ref. [40] a numerical study was performed that showed how the mechanics of a processive motor protein gets more complicated if the noise from the bath is Lévy distributed. Above, a more basic and general mechanism has been described analytically.

Many ailments are associated with the misfolding of proteins. Chaperones assist in the correct folding of proteins and part of their operation is the catalysis of steps leading to the correct folding. Alzheimer’s, Parkinson’s, and cystic fibrosis are examples of diseases that can occur when protein folding or unfolding is not properly chaperoned. The epicatalysis mechanism could be important for a better understanding of such disorders. Prions are misfolded proteins that catalyze identical misfolding of proteins with the same primary structure [41]. Prions are the infectious agents of well-known ailments such as mad cow disease, Creutzfeldt-Jacob disease, and kuru. In a nonequilibrium environment a stronger autocatalytic, positive-feedback cycle for the production of prions could actually occur through the effect described in this article.

The catalytic networks involving DNA, RNA, and proteins are often quite complicated. The insights we have developed above add a hitherto unrecognized effect and an extra complication. However, this new understanding may also help in the design of new ways of therapeutic intervention.

- 
- [1] H. Risken, *The Fokker-Planck Equation* (Springer, Berlin, 1989).
  - [2] N. G. van Kampen, *Stochastic Processes in Physics and Chemistry* (Elsevier, Amsterdam, 1992).
  - [3] J. B. Johnson, *Phys. Rev.* **26**, 71 (1925).
  - [4] B. Mandelbrot, *J. Bus.* **36**, 394 (1963).
  - [5] C.-K. Peng, J. Mietus, J. M. Hausdorff, S. Havlin, H. E. Stanley, and A. L. Goldberger, *Phys. Rev. Lett.* **70**, 1343 (1993).
  - [6] T. J. P. Penna, P. M. C. de Oliveira, J. C. Sartorelli, W. M. Gonçalves, and R. D. Pinto, *Phys. Rev. E* **52**, R2168(R) (1995).
  - [7] G. Boffetta, V. Carbone, P. Giuliani, P. Veltri, and A. Vulpiani, *Phys. Rev. Lett.* **83**, 4662 (1999).
  - [8] C. Battle, C. P. Broedersz, N. Fakhri, V. F. Geyer, J. Howard, C. F. Schmidt, and F. C. MacKintosh, *Science* **352**, 604 (2016).
  - [9] H. Turlier, D. A. Fedosov, B. Audoly, T. Auth, N. S. Gov, C. Sykes, J.-F. Joanny, G. Gompper, and T. Betz, *Nat. Phys.* **12**, 513 (2016).
  - [10] B. Mandelbrot, *The Fractal Geometry of Nature* (W. H. Freeman, San Francisco, 1983).
  - [11] S. Chandrasekhar, *Rev. Mod. Phys.* **15**, 1 (1943).

- [12] B. V. Gnedenko and A. N. Kolmogorov, *Limit Distributions for Sums of Random Variables* (Addison-Wesley, Cambridge, MA, 1954).
- [13] J. Klafter, M. F. Shlesinger, and G. Zumofen, *Phys. Today* **49**(2), 33 (1996).
- [14] K. Górska and K. A. Penson, *Phys. Rev. E* **83**, 061125 (2011).
- [15] G. E. Crooks, *J. Stat. Mech.* (2011) P07008.
- [16] L. Onsager and S. Machlup, *Phys. Rev.* **91**, 1505 (1953).
- [17] M. Bier and R. D. Astumian, *Phys. Lett. A* **247**, 385 (1998).
- [18] M. Bier, I. Derényi, M. Kostur, and R. D. Astumian, *Phys. Rev. E* **59**, 6422 (1999).
- [19] Ł. Kuśmierz, A. V. Chechkin, E. Gudowska-Nowak, and M. Bier, *Europhys. Lett.* **114**, 60009 (2016).
- [20] P. Imkeller and I. Pavlyukevich, *J. Phys. A* **39**, L237 (2006).
- [21] L. Pauling, *General Chemistry* (Dover, New York, 1988).
- [22] D. P. Sheehan, *Phys. Rev. E* **88**, 032125 (2013).
- [23] D. P. Sheehan, D. J. Mallin, J. T. Garamella, and W. F. Sheehan, *Found. Phys.* **44**, 235 (2014).
- [24] *Maxwell's Demon 2 - Classical and Quantum Information, Computing*, edited by H. S. Leff and A. F. Rex (Institute of Physics Publishing, Bristol, UK, 2003).
- [25] D. Kondepudi and I. Prigogine, *Modern Thermodynamics: From Heat Engines to Dissipative Structures* (Wiley, New York, 1998).
- [26] P. D. Ditlevsen, *Phys. Rev. E* **60**, 172 (1999).
- [27] J. B. Bassingthwaighe, L. S. Liebovitch, and B. J. West, *Fractal Physiology* (Oxford University Press, New York, 1994).
- [28] C. Wilhelm, *Phys. Rev. Lett.* **101**, 028101 (2008).
- [29] F. Gallet, D. Arcizet, P. Boheca, and A. Richerta, *Soft Matter* **5**, 2947 (2009).
- [30] M. Guo, A. J. Ehrlicher, M. H. Jensen, M. Renz, J. R. Moore, R. D. Goldman, J. Lippincott-Schwartz, F. C. Mackintosh, and D. A. Weitz, *Cell* **158**, 822 (2014).
- [31] M. S. e Silva, B. Stuhmann, T. Betz, and G. H. Koenderink, *New J. Phys.* **16**, 075010 (2014).
- [32] R. Jha, P. K. Kaw, D. R. Kulkarni, J. C. Parikh, and ADITYA Team, *Phys. Plasmas* **10**, 699 (2003).
- [33] K. Burnecki, A. Wyłomańska, A. Beletskii, V. Gonchar, and A. Chechkin, *Phys. Rev. E* **85**, 056711 (2012).
- [34] W. Ebeling and M. Yu. Romanovsky, *Contrib. Plasma Phys.* **49**, 477 (2009).
- [35] J. Zweiback, T. E. Cowan, R. A. Smith, J. H. Hartley, R. Howell, C. A. Steinke, G. Hays, K. B. Wharton, J. K. Crane, and T. Ditmire, *Phys. Rev. Lett.* **85**, 3640 (2000).
- [36] E. G. Adelberger, A. García, R. G. H. Robertson *et al.*, *Rev. Mod. Phys.* **83**, 195 (2011).
- [37] S. E. Jones, A. N. Anderson, A. J. Caffrey *et al.*, *Phys. Rev. Lett.* **56**, 588 (1986).
- [38] L. I. Ponomarev, *Contemp. Phys.* **31**, 219 (1990).
- [39] K. Neupane, D. B. Ritchie, H. Yu, D. A. N. Foster, F. Wang, and M. T. Woodside, *Phys. Rev. Lett.* **109**, 068102 (2012).
- [40] B. Lisowski, D. Valenti, B. Spagnolo, M. Bier, and E. Gudowska-Nowak, *Phys. Rev. E* **91**, 042713 (2015).
- [41] M. Eigen, *Biophys. Chem.* **63**, A1 (1996).